Electronic Supplementary Material (ESI) for Nanoscale.
This journal is © The Royal Society of Chemistry 2015

# Supplementary Information

# Design, Fabrication and Charge Recombination Analysis of Interdigitated Heterojunction Nanomorphology on P3HT/$PC_{70}$BM Solar Cells

Victor S. Balderrama,[a,b] Josep Albero,[c] Pedro Granero,[a] Josep Ferré-Borrull,[a] Josep Pallarés,[a] Emilio Palomares[d,e] and Lluis F. Marsal *[a]

[a]Departament d'Enginyeria Electrònica, Elèctrica i Automàtica, University of Rovira i Virgili, Països Catalans 26, 43007 Tarragona, Spain,

[b]Sección de Electrónica del Estado Sólido, Departamento de Ingeniería Eléctrica, CINVESTAV, Av. IPN No. 2508, 07360, D.F., Mexico

[c]Institute of Chemical Technology of Valencia (ITQ) Avenue De los Naranjos s/n, 46022 Valencia, Spain

[d]Institute of Chemical Research of Catalonia (ICIQ) Països Catalans 24, 43007 Tarragona, Spain

[e] ICREA. Passeig Lluís Companys, 23, 08010 Barcelona, Spain

## SI-1. Fabrication conditions of NAAT

The samples of nanoporous anodic alumina template (NAATs) were fabricated in two-step anodization process. **Table S1** summarizes the fabrication conditions.

TABLE S1. Fabrication Conditions of the NAAT

| | oxalic acid | $V_{anod}$ [a] (V) | $t_{anod}$ (1st step) [b] (h) | $t_{anod}$ (2nd step) (s) | $t_{pw}$ [c] (min) |
|---|---|---|---|---|---|
| Template | $H_2C_2O_4$ (0.3 M) | 40 | 24 | 60 | 14 |

[a] $V_{anod}$ is anodization voltage. [b] $t_{anod}$ is anodization time. [c] $t_{pw}$ is pore-widening time.

## SI-2. Geometric characteristics of NAAT

The geometric characteristics of the resulting NAAT were got from ESEM image and **Table S2** summarizes the values.

TABLE S2. Geometric Characteristics of NAAT

| | $\phi_p$ [a] (nm) | $H_p$ [b] (nm) | $d_{int}$ [c] (nm) |
|---|---|---|---|
| Template of NAA (twenty samples) | 60 ± 4 | 80 ± 5 | 100 ± 4 |

[a] $\phi_p$ is pore diameter. [b] $H_p$ is pore height. [c] $d_{int}$ is interpore distance.

Figure S1 shows a physical sample of NAAT and the geometric characteristics.

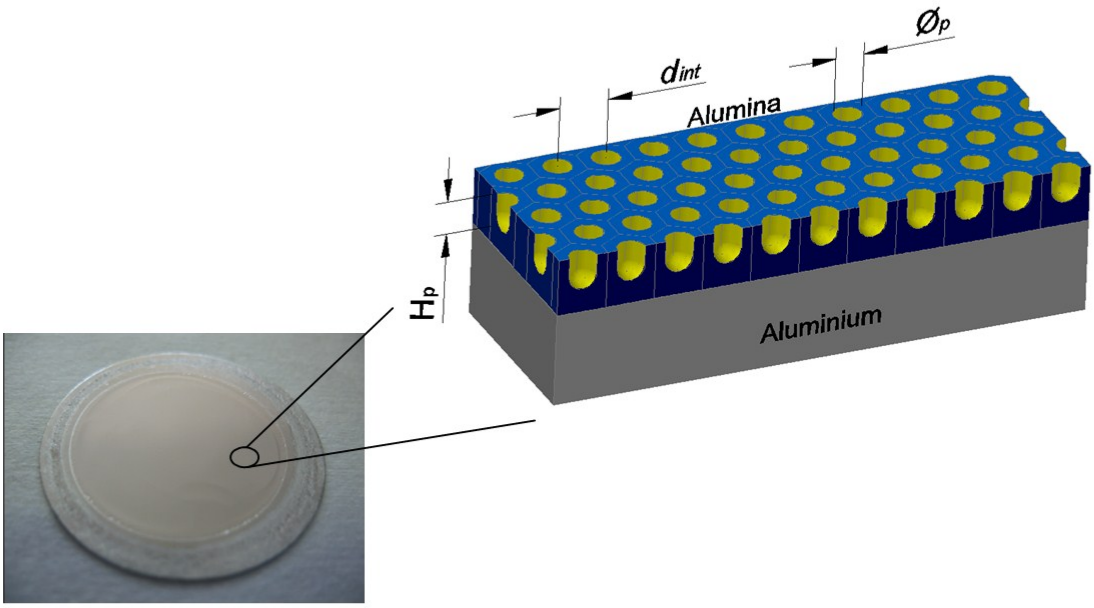


**Fig. S1** NAAT shows all its geometric characteristics.

## SI-3. NAAT ESEM images

The characteristics of the resulting NAAT were got from ESEM image under different views.

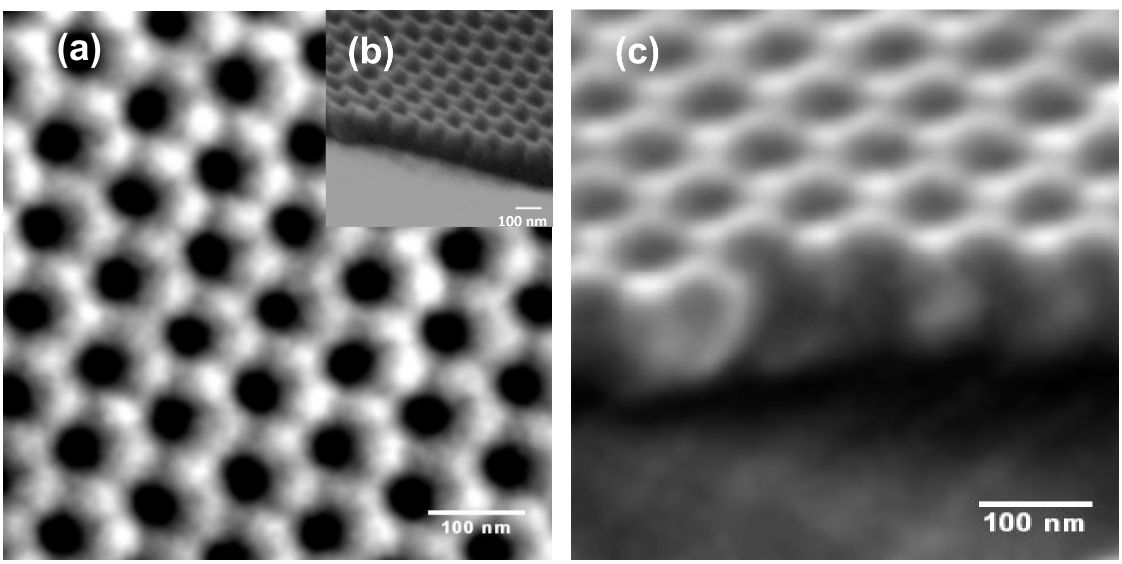

**Fig. S2** ESEM images of NAAT. (a) Top-view, (b) tilt-view and (c) cross section-view of NAAT. The geometrical characteristics were: $\phi_{pore} = 60 \pm 4$ nm, $H_{pore} = 80 \pm 5$ nm and $d_{inter} = 100 \pm 4$ nm.

## SI-4. AFM images

**Fig. S3 a, d** and **g** show the topography images of P3HT–NP revealing a periodically structured top surface with an average nanopillar height of ~ 80 nm and interpillar distance ~100 nm as was seen in the ESEM images. P3HT:$PC_{70}$BM–BHJ has an average surface height of 13.39 nm and the P3HT–single layer has an average surface height of 23 nm, respectively. **Fig. S3 b, e** and **h** are shown the phase image and **Fig. S3 c, f** and **I** are shown the tilt view of the P3HT–NP, P3HT:$PC_{70}$BM–BHJ and P3HT–single layer, respectively.

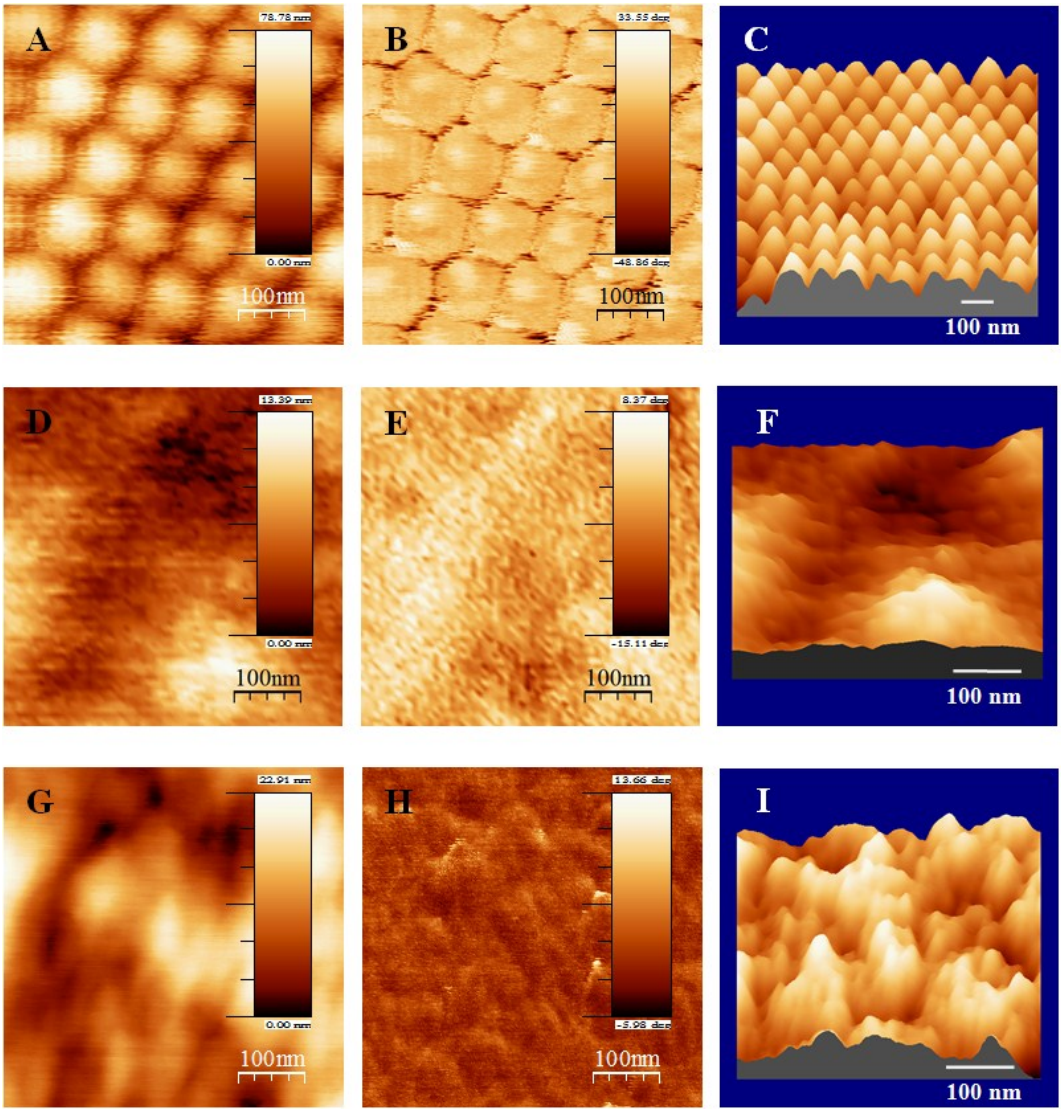


**Fig. S3** (a, b, c) AFM morphology, phase and tilt view images of the P3HT–NP layer after soft nanoimprinting by NAAT. (d, e, f) AFM morphology, phase and tilt view images of the P3HT:$PC_{70}BM$–BHJ layer after spin coating deposition. (g, h, i) AFM morphology, phase and tilt view images of the P3HT–single layer after spin coating deposition. All the layers underwent thermal annealing at T = 130$^{o}$C for t = 20 min.

**SI-5. PL measurements**

**Fig. S4** shows the PL measurement for nanopillar samples and it was 16% greater in intensity than P3HT–flat film at 695 nm. On the other hand, after PL quenching the intensity of P3HT–

NP/$PC_{70}$BM–IHJN film was 94.8% lower than that of pure of P3HT–NP at 695 nm. For P3HT:$PC_{70}$BM–BHJ film and P3HT/$PC_{70}$BM–BL film the PL quenching was observed to be 85.3% and 92.7% lower than that of P3HT–flat film at 695 nm, respectively.

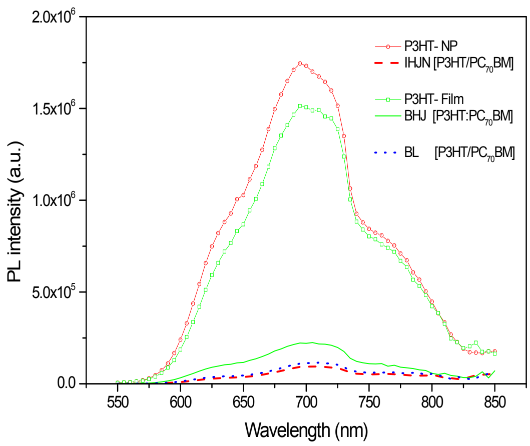


**Fig. S4** (Color on line) Photoluminescence spectres were obtained from P3HT nanopillars (red open circles) and P3HT– single film (green open squares). The same graph shows the PL spectrums from IHJN–[P3HT/$PC_{70}$BM] (red dashed line), BHJ–[P3HT:$PC_{70}$BM] (green continuous line) and BL–[P3HT/$PC_{70}$BM] (blue dotted line). The excitation wavelength was applied at 510 nm.

The best PL quenching of the three structures was for P3HT/$PC_{70}$BM–IHJN film. The total quenching of PL emission between the interfaces of polymer-fullerene might indicate that there is an efficient photoinduced and charge transfer at the interfaces of P3HT/$PC_{70}$BM materials.[1, 2] Therefore, on the P3HT–NP nanomorphology the interpillar distance between two nanopillar walls was 40 nm (maximum distance to D/A interface: 20 nm).This geometry may help the excitons to diffuse more easily at the polymer/fullerene composite interface (as it is well known that the exciton diffusion length is ~10 nm in P3HT[3, 4]), which improves the performance parameters of the cells. By integrating the area below the PL spectra the electron injection yield from P3HT to $PC_{70}$BM can be estimated. In P3HT/$PC_{70}$BM–IHJN film, P3HT:$PC_{70}$BM–BHJ film and P3HT/$PC_{70}$BM–BL film these yields were 95%, 86% and 92%, respectively.

## References


1. X. He, F. Gao, G. Tu, D. G. Hasko, S. Hüttner, N. C. Greenham, U. Steiner, R. H. Friend and W. T. S. Huck, *Adv. Funct. Mater.* , **2011**, 21, 139-146.
2. J. S. Kim, Y. Park, D. Y. Lee, J. H. Lee, J. H. Park, J. K. Kim and K. Cho, *Adv. Funct. Mater.* , **2010**, 20, 540-545.
3. C. W. Tang and S. A. Vanslyke, *Appl. Phys. Lett.*, **1987**, 51, 913-915.
4. J. Slota, X. Hea and W. T. S. Huck, *Nano Today*, **2010**, 5, 231-241.